Design and Simulation of Closed-Loop Ground Alignment of Inertial Platforms with Sway Motion

S. Vathsal*
NASA Goddard Space Flight Center, Greenbelt, Maryland

This paper is concerned with the application of optimal estimation and control concepts to the ground alignment of inertial platforms subjected to random sway motion. A seventh-order Kalman filter has been designed for estimating the platform misalignments and sway motion. Using the linear quadratic optimal regulator techniques, feedback controller gains have been designed to drive the initial misalignments to a small value. A reconfiguration of the filter controller scheme has been proposed and verified by Monte Carlo simulation for improving the speed of alignment without changing the alignment accuracy.

I. Introduction

PRELAUNCH alignment or ground alignment of inertial platforms has assumed a great deal of importance in the design of inertial navigation systems.[1] Gyro compassing principles have long been applied to this problem; this application is known as the conventional mode of alignment and calibration.[2-4] There exists an operational state-of-the-art in aircraft and shipboard inertial navigators, all of which must be aligned using some variation of gyro compassing.

In order to navigate an aircraft to an overall accuracy of 1 n. mi/h, it is desirable to limit the initial azimuth error to 5 arc min and the initial tilt to 20 arc sec.[17] For a platform used in a carrier deck, the alignment needs to be carried out in a much shorter time. Naturally, these accuracy and alignment-time requirements have demanded the application of Kalman filtering techniques. The alignment schemes with the Kalman filter can be either an open-loop or a closed-loop scheme. Many investigators have explored the open-loop alignment in detail.[6-8] Jurenka and Leondes[5] have considered the optimum alignment of an inertial autonavigator; their performance criterion has been to minimize only the mean square azimuth error. They have chosen the controls in such a way that the inputs to the integrators of the states are zero. Their control law cannot drive the initial misalignments to a small value, as required by closed-loop alignment. Winter[9] has derived the modeling error sensitivity equations. Stieler and Zenz[10] have considered both open-loop and closed-loop alignment using both gyro compassing techniques and Kalman filter. The authors[10] achieved closed-loop alignment by setting control gains designed by heuristic arguments rather than by using optimal control techniques. It is often noted that the gyro compass does not perform very well in the presence of long-period sway motions during ground alignment.[10] Hence, it is necessary to model them and add in the state vector and see whether the filter would identify the sway motion.

In the conventional gyro compass, the speed of alignment can be improved to some extent by designing the gyro-compassing loop gains. Accuracy of alignment depends on the external noise and sway motion. On the other hand, the Kalman filter can improve the alignment accuracy, provided the noise statistics are known. If the filter is used in the open-loop mode, the gyro torquers are activated only after the filter attains a steady state. In the closed-loop mode, the feedback signals are continuously fed to the platform as well as to the filter. Hence the estimation error, which is a measure of the alignment accuracy, is the same for both open- and closed-loop alignment. However, by a reconfiguration of the filter as proposed in Ref. 14, different speeds of alignment could be achieved for the same Kalman filter alignment accuracy for both open- and closed-loop alignment. In this paper, the platform alignment problem has been formulated as a closed-loop estimation and control problem. The following specific aspects have been considered:

1) Design of feedback control gains using optimal regulator techniques by solving the matrix Riccati equation.
2) Modeling of aircraft sway using an experimental autocorrelation function and incorporation of the dynamic model into the filter.
3) Gyro-drift rates identification.
4) Suitable reconfiguration of the filter for faster alignment.

Though the platform dynamics is nonlinear, small angle approximation can be made to linearize the platform dynamics. Then, by separation theorem, the estimator and controller can be designed independently. The feedback torquer signals obtained by this method may lead to large torquer rates, which cannot be applied due to hardware design constraints. This aspect has been incorporated into the simulation by a saturation type of nonlinearity.

Section II deals with the problem formulation. Section III is concerned with the reconfiguration of the filter for speeding up the alignment. The platform error model and the model for aircraft sway have been derived in Sec. IV. Filter and controller design is given in Sec. V. Simulation results are summarized in Sec. VI.

II. Formulation of Closed-Loop Alignment of Inertial Platforms

A general schematic for closed-loop alignment of platforms has been given in Fig. 1. The platform dynamics, the sensor errors, and the sway acceleration of the base can be described by the following n-dimensional linear system.

$$\dot{x} = Fx + Bu + Gw \tag{1}$$

where F, B, and G are constant matrices, w is a white-noise vector that represents the gyro-drift rates, and x is the state vector that represents the north, east, and vertical misalignments of the platform augmented with the states depicting the sway motion of the base. The vector u denotes the gyro-torquer feedback signals, which can be generated by multiplying the estimated state vector x with the control matrix Γ^* as follows:

$$u = -\Gamma^* x \tag{2}$$

Received Feb. 14, 1985; revision received July 15, 1985.

*National Research Council–NASA Research Associate.

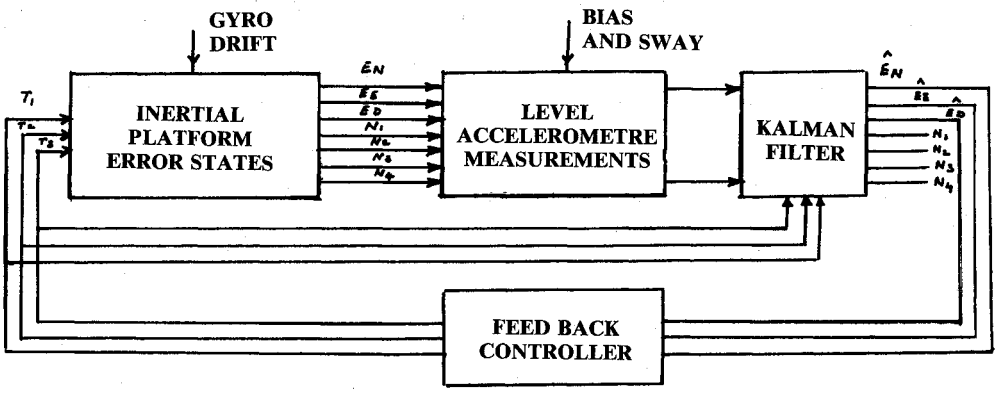

Fig. 1 Schematic for closed-loop alignment of platforms.

If the platform is kept stationary in the ground, the north accelerometer measures the east misalignment, the north accelerometer bias, and the sway acceleration in the north-south direction. Similarly, the east accelerometer measures the north misalignment, the east accelerometer bias, and the sway acceleration in the east-west direction. The m-dimensional measurement vector z can be modeled as

$$z = Hx + v \tag{3}$$

H is a constant measurement matrix, and v is a vector of white noise representing the measurement errors. The system noise w and the measurement noise v are assumed to be uncorrelated with each other. Without any loss of generality, w and v are assumed to be zero mean white-noise processes

$$E[w(t)] = 0, \quad E[v(t)] = 0, \quad E[w(t)v^T(\tau)] = 0$$
$$E[w(t)w^T(\tau)] = Q\delta(t-\tau), \quad E[v(t)v^T(\tau)] = R\delta(t-\tau) \tag{4}$$

where $E(\cdot)$ is the expected value and $\delta(t)$ is the Dirac delta function. The matrices Q and R can be derived from the noise covariance data. The measurement vector z is used to construct the Kalman-Bucy filter,[16] which is a linear unbiased estimator of the form

$$\dot{\hat{x}} = (F - K^*H)\hat{x} + K^*z + Bu \tag{5}$$

where K^* is the $(n \times m)$ gain matrix that can be generated from

$$K^* = PH^TR^{-1} \tag{6}$$

and P is the error covariance matrix defined as

$$P = E\left[(x - \hat{x})(x - \hat{x})^T\right] \tag{7}$$

Matrix P can be propagated using the matrix Riccati equation

$$\dot{P} = FP + PF^T - PH^TR^{-1}HP + Q, \; P(t_0) = P_0 \tag{8}$$

Equation (8) can be solved forward in time. P_0 is the covariance matrix of initial errors of the platform.

Implicit in this formulation is the assumption that $x(t_0)$ is a zero mean random vector, which represents the initial misalignments. It follows that

$$E[x(t_0)x^T(t_0)] = P_0 \tag{9}$$

In ground alignment of inertial platform, if the platform is maintained level, the initial azimuth misalignment needs to be estimated and controlled. In general, the north, east, and azimuth misalignments need to be estimated and controlled. In practice, P_0 can be generated from the accuracy attainable in a coarse alignment prior to the fine closed-loop alignment to be carried out using the Kalman filter. Since the initial misalignments need to be driven to zero or, in practice, to a small value as required by the mission, the feedback control matrix can be obtained using optimal control techniques.

Control Matrix Γ^* is given by

$$\Gamma^* = R_c^{-1}B^T\Sigma_c \tag{10}$$

where

$$\dot{\Sigma}_c = -F^T\Sigma_c - \Sigma_c F + \Sigma_c BR_c^{-1}B^T\Sigma_c - Q_c, \; \Sigma_c(t_7) = \Sigma_{c7} \tag{11}$$

Q_c and R_c are weightage matrices used to minimize the quadratic performance index $J_c(u)$ given by

$$J_c(u) = \int_{t_0}^{t_f}\left[x^TQ_cx + u^TRu\right]dt + x^T\Sigma_{c7}x|_{t=t_7} \tag{12}$$

where t_0 and t_f define the alignment interval. Matrix Σ_c can be obtained by solving the matrix Riccati equation given by Eq. (11) backward in time. The application of the Kalman filter and optimal control techniques demands that R and R_c be positive definite matrices and that Q and Q_c be at least positive semidefinite. Section III describes the reconfiguration of the filter for speeding up the alignment.

III. Filter Reconfiguration for Varying Speed of Alignment

Denoting $\tilde{x}$ as the estimation error, from Eqs. (1), (3), and (5), it follows that

$$\dot{\tilde{x}} = (F - KH)\tilde{x} + Gw - Kv \tag{13}$$

where $\tilde{x} = x - \hat{x}$. The estimation error propagation is independent of the control signal. Instead of the conventional form of the filter, one can design a new filter $\hat{x}_n$ given by

$$\dot{\hat{x}}_n = (F - K_f^*H)\hat{x}_n + K^*z - B\Gamma^*\hat{x}_n \tag{14}$$

where K^* is the optimal gain corresponding to the real-world model and K_f^* is any suboptimal gain of the filter corresponding to a lower-order model. Then, in order to get the same estimation error covariance of the Kalman filter, it is necessary to feed $-(K_f^* - K^*)H\hat{x}_n$ into the real-world system. The theoretical justification for this type of reconfiguration is available in Ref. 14. This idea can be utilized for obtaining different speeds of alignment. Let

$$\Gamma_c = -(K_f^* - K^*)H\hat{x} \tag{15}$$

Then, the real-world system becomes

$$\dot{x}_n = Fx_n - B\Gamma^*\hat{x}_n + Gw + \Gamma_c \tag{16}$$

Subtracting Eq. (14) from Eq. (16), one gets

$$\dot{x}_n - \dot{\hat{x}}_n = \dot{\tilde{x}}_n = (F - K^*H)\tilde{x}_n + Gw - K^*v \tag{17}$$

from Eqs. (13) and (17), it follows that

$$\mathrm{cov}[\tilde{x}_n] = \mathrm{cov}[\tilde{x}] \tag{18}$$

where $\tilde{x}_n = x_n - \hat{x}_n$, provided the initial covariance is the same. In a practical situation, they need not be the same. The convergence characteristics of the filter given in Eq. (14) are different from the conventional structure given by Eq. (5). The speed of alignment can be controlled by changing the eigenvalues of $(F - K_I^*H - B\Gamma^*)$ through K_I^* and Γ^*, independently. The actual simulation layout that illustrates this fact is shown in Sec. VI.

IV. Derivation of Platform Error Model and Sway Motion

A rigorous, detailed error model of the real-world inertial system contains 50 or more error states. However, the error sensitivity studies reported by Winter[9] indicate that only 13 states are really significant as far as the ground alignment filter is concerned. If one assumes a white-noise model for gyro drifts, then the system could be represented by a seven-state model containing the three platform misalignments. Though the white-noise representation is quite simple for the gyro drift, while including the sway motion, the drift-rate states need not be precisely modeled. The switch on uncertainty of gyro drifts can be modeled as random biases. Then a sixth-order model can be constructed to identify the drifts as shown in Eq. (30). The details are available in Ref. 11. The dynamic model for the misalignments is derived here from fundamentals based on Ref. 7.

Assume that the platform is misaligned from the reference system by a small angle $\theta = [E_N, E_E, E_D]$, as shown in Fig. 2. The reference system corresponds to north, east, and vertical. Since X_0 is defined as locally vertical, a measurement of acceleration along axes Z and Y is proportional to the misalignment angles E_N and E_E. While the reference coordinates rotate exactly at Earth's rotational rates, the platform cannot be torqued since the misalignment angles E_N, E_E, and E_D are not known. This causes these angles to vary with time due to Earth's rate coupling. Additionally, the angles change due to the error drift rate of the gyros. The level accelerometers sense not only the misalignments but also the sway motion.

The three coordinate systems needed for the derivation of the error model are: 1) Earth-fixed launch site coordinates CS (0), 2) platform reference coordinates CS (1), and 3) platform instrument coordinate CS (2).

If W_2 is the matrix of angular rates measured by the gyros, then

$$W_2 = \dot{\theta} + d_2 \tag{19}$$

If W_0 is the matrix of Earth's rate in CS (0), then

$$\frac{\mathrm{d}}{\mathrm{d}t}(1_{C_2}) = 1_{C_2}W_2 - W_0 1_{C_2} \tag{20}$$

Equation (20) is derived from fundamentals in Ref. 7. Matrix d_2 represents the gyro-drift rates in the instrument axes. The inverse equation to Eq. (20) is

$$\frac{\mathrm{d}}{\mathrm{d}t}(2_{C_1}) = 2_{C_1}W_0 - W_2 2_{C_1} \tag{21}$$

Substituting for W_2 from Eq. (19),

$$\frac{\mathrm{d}}{\mathrm{d}t}(2_{C_1}) = 2_{C_1}W_0 - \dot{\theta}2_{C_1} - d_2 2_{C_1} \tag{22}$$

$$0_{C_1} = 0_{C_2}2_{C_1} \tag{23}$$

Matrix 0_{C_1} is the transformation matrix from CS (0) to CS (1). Differentiating Eq. (23), one gets

$$\frac{\mathrm{d}}{\mathrm{d}t}(0_{C_1}) = 0_{C_2}2_{C_1}W_0 - 0_{C_2}\dot{\theta}2_{C_1} - 0_{C_2}d_2 2_{C_1} + \frac{\mathrm{d}}{\mathrm{d}t}(0_{C_2})2_{C_1} \tag{24}$$

Same as Eq. (20)

$$\frac{\mathrm{d}}{\mathrm{d}t}(0_{C_2}) = 0_{C_2}\dot{\theta} - W_0 0_{C_2} \tag{25}$$

Substituting Eq. (25) into Eq. (24) yields

$$\frac{\mathrm{d}}{\mathrm{d}t}(0_{C_1}) = 0_{C_1}W_0 - W_0 0_{C_1} - 0_{C_2}d_2 0_{C_1} \tag{26}$$

Components of drift will be assumed constant in CS (1) rather than CS (2).

Since CS (1) differs from CS (0) by small angles E_N, E_E, E_D, matrix 0_{C_1} can be written as

$$0_{C_1} = \begin{bmatrix} 1 & + & E_E & - & E_N \\ -E_E & & 1 & + & E_D \\ +E_N & & -E_D & & 1 \end{bmatrix} \tag{27}$$

Substituting Eq. (27) into Eq. (26) yields only three equations, since the angles on E_N, E_E, E_D, are small. The drift terms can be written as

$$0_{C_2}d_2 2_{C_1} = 0_{C_1}1_{C_2}d_2 2_{C_1} = 0_{C_1}d_1 \tag{28}$$

Finally, simplification of Eq. (26) yields

$$\begin{bmatrix} \dot{E}_N \\ \dot{E}_E \\ \dot{E}_D \end{bmatrix} = \begin{bmatrix} 0 & -\Omega\sin\phi & 0 \\ \Omega\sin\phi & 0 & \Omega\cos\phi \\ 0 & -\Omega\cos\phi & 0 \end{bmatrix} \begin{bmatrix} E_N \\ E_E \\ E_D \end{bmatrix} + \begin{bmatrix} d_N \\ d_E \\ d_D \end{bmatrix} \tag{29}$$

where $[d_2] = [d_N \quad d_E \quad d_D]^T$, Ω is Earth rate, and ϕ is the latitude of alignment. If the drift rates are assumed as random

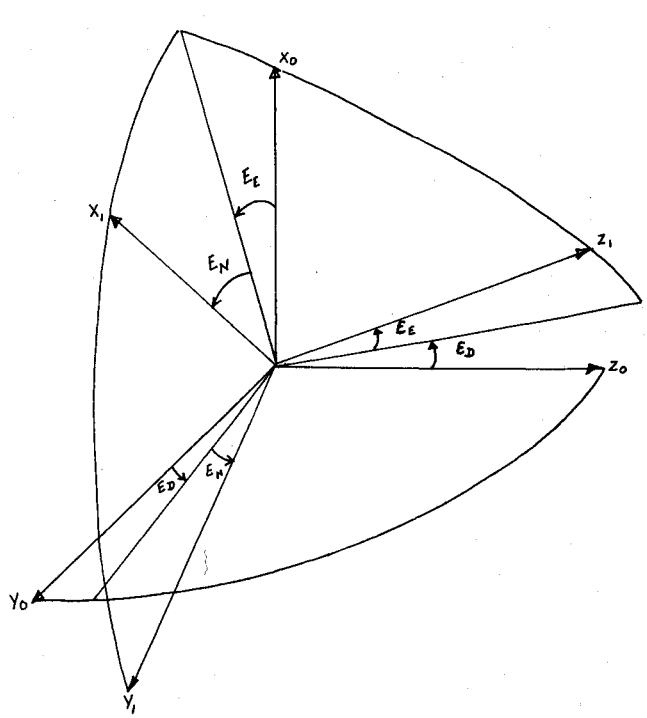

Fig. 2 Coordinate system for platform misalignments.

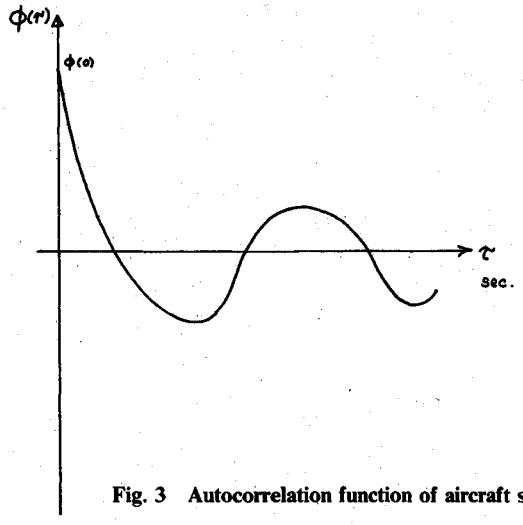

Fig. 3 Autocorrelation function of aircraft sway.

biases, then

$$\begin{bmatrix} \dot{E}_N \\ \dot{E}_E \\ \dot{E}_D \\ \dot{d}_N \\ \dot{d}_E \\ \dot{d}_D \end{bmatrix} = \begin{bmatrix} 0 & -\Omega\sin\phi & 0 & 1 & 0 & 0 \\ \Omega\sin\phi & 0 & \Omega\cos\phi & 0 & 1 & 0 \\ 0 & -\Omega\cos\phi & 0 & 0 & 0 & 1 \\ 0 & 0 & 0 & 0 & 0 & 0 \\ 0 & 0 & 0 & 0 & 0 & 0 \\ 0 & 0 & 0 & 0 & 0 & 0 \end{bmatrix} \begin{bmatrix} E_N \\ E_E \\ E_D \\ d_N \\ d_E \\ d_D \end{bmatrix} \tag{30}$$

From Eq. (30), drift rates can be identified.[11] The level accelerometers measure the acceleration due to gravity proportional to E_N and E_E

$$Z_1 = -gE_N + b_E + N_1 \tag{31}$$

$$Z_2 = gE_E + b_N + N_3 \tag{32}$$

where b_E and b_N correspond to east and north accelerometer biases and N_1 and N_3 are the sway acceleration.

Modeling of sway is beset with practical difficulties. For the DFVLR test aircraft HFB 320, sway has been measured experimentally, and an autocorrelation function has been worked out as shown in Fig. 3. The details of the sway measurement can be found in Ref. 18. The sway motion of HFB 320 is low frequency because it is a test aircraft. From Fig. 3, it is clear that the random sway exhibits periodic behavior. The autocorrelation function model derived in Ref. 18 is given by

$$\phi_{x_1,x_1}(\tau) = \sigma^2 e^{-\beta|\tau|}\cos w|\tau| \tag{33}$$

where the values of σ^2, β, and w are chosen on the basis of the physics of the situation or to fit the empirical autocorrelation data. Two state variables are necessary to represent a random variable with this autocorrelation function.[16,19] One pair of quantities that provides this relation obeys the following differential equations.[19]

$$\begin{aligned} \dot{N}_1 &= N_2 + w_{s_1} \\ \dot{N}_2 &= -\alpha_1^2 N_1 - 2\beta_1 N_2 + (\alpha_1 - 2\beta_1) w_{s_1} \end{aligned} \tag{34}$$

where

$$\alpha = (\beta^2 + w^2)^{\frac{1}{2}} \tag{35}$$

The spectral density of the white-noise w_{s_1} is $2\beta\sigma_1^2$. The derivation of the second-order shaping filters is given in the Appendix. For the DFVLR test aircraft HFB 320, the following parameters have been worked out. $\phi(0) = \sigma_1^2 = 1.86 \times 10^{-6}$ m^2/sec^4; $\xi_1 = 0.7$; $f_1 = .0053$ Hz; $\alpha_1 = 3.33 \times 10^{-2}$ rad/sec.

V. Design of Filter and Controller

The error model of the platform normally contains the three misalignment angles E_N, E_E, and E_D as state variables. The sway in both the north and east directions constitutes four additional states to be added to the platform error model.

The real-world state vector x can be defined as

$$x = [E_N, E_E, E_D, N_1, N_2, N_3, N_4]^T \tag{36}$$

where N_3 and N_4 are derived in the same way as N_1 and N_2, respectively. The parameters needed to represent N_3 and N_4 are denoted by $\sigma_2, \alpha_2, \beta_2$. In the present study, it has been assumed that $\sigma_1 = \sigma_2$, $\alpha_1 = \alpha_2$, and $\beta_1 = \beta_2$. The F matrix takes the following form:

$$F = \left[\begin{array}{ccccccc} 0 & -\Omega\sin\phi & 0 & 0 & 0 & 0 & 0 \\ \Omega\sin\phi & 0 & \Omega\cos\phi & 0 & 0 & 0 & 0 \\ 0 & -\Omega\cos\phi & 0 & 0 & 0 & 0 & 0 \\ 0 & 0 & 0 & 0 & 1 & 0 & 0 \\ 0 & 0 & 0 & -\alpha_1^2 & -2\beta_1 & 0 & 0 \\ 0 & 0 & 0 & 0 & 0 & 0 & 1 \\ 0 & 0 & 0 & 0 & 0 & -\alpha_2^2 & -2\beta_2 \end{array}\right] \tag{37}$$

The state noise vector w is given by

$$w = [d_N, d_E, d_D, w_{s_1}, (\alpha_1 - 2\beta_1) w_{s_1}, w_{s_2}, (\alpha_2 - 2\beta_2) w_{s_2}]^T$$

Here, d_N, d_E, and d_D denote the gyro-drift rates modeled as white random noise. Ω is the Earth rate, and ϕ is the latitude of alignment, which is constant for the ground alignment. Ω and ϕ are given by $\Omega = 7.29 \times 10^{-5}$ rad/sec; $\phi = 52.317$ deg, the latitude of Braunschweig, West Germany. The matrix H and vector v are given by

$$H = \begin{bmatrix} -g & 0 & 0 & 1 & 0 & 0 & 0 \\ 0 & g & 0 & 0 & 0 & 1 & 0 \end{bmatrix}, \quad v = [b_E, b_N]^T \tag{38}$$

where b_E and b_N are the accelerometer biases modeled as white measurement noise.

From the sensor error specifications supplied by the sensor manufacturer, the following values have been chosen for the noise covariance matrices and initial state uncertainty. Specifically, Q, R, and P_0 are given as follows: covariances Q and R are diagonal matrices whose diagonal elements are given below.

$$\begin{aligned} Q_{11} &= Q_{22} = Q_{33} = 4.25 \times 10^{-15} \text{ sec}^{-1} \\ Q_{N_1N_1} &= Q_{N_3N_3} = 8.91 \times 10^{-8} \text{ m}^2/\text{sec}^3 \\ Q_{N_2N_2} &= Q_{N_4N_4} = 3.3 \times 10^{-10} \text{ m}^2/\text{sec}^3 \\ R_{11} &= R_{22} = 9.6 \times 10^{-8} \text{ m}^2/\text{sec}^3 \end{aligned} \tag{39}$$

Since the initial level misalignments are very small, they can be treated as zero. Azimuth misalignment E_D is rather large, of the order of 100 mrad. Hence, in the P_0 matrix, all the elements other than P_{33} can be set to zero; P_{33} can be set to $(.01)^2$(rad)^2. The design has also been carried out for an initial level error of 2 mrad, a realistic figure normally employed. For the system under consideration, the Kalman filter designed is seventh order; its gains, defined by Eq. (6), have been computed by solving the continuous matrix Riccati equation.

Table 1 Optimal control gains for closed-loop alignment

Time, s	Control gains for closed-loop alignment, (rad/s)/rad								
	Γ_{11}^*	Γ_{12}^*	Γ_{13}^*	Γ_{21}^*	Γ_{22}^*	Γ_{23}^*	Γ_{31}^*	Γ_{32}^*	Γ_{33}^*
0	1.2247	0.40817×10^{-3}	0.40820×10^{-3}	0.40817×10^{-3}	1.2247	0.40817×10^{-3}	0.40820×10^{-3}	0.40817×10^{-3}	1.2247
↓	↓	↓	↓	↓	↓	↓	↓	↓	↓
505	1.2247	0.40817×10^{-3}	0.40819×10^{-3}	0.40817×10^{-3}	1.2247	0.40817×10^{-3}	0.40819×10^{-3}	0.40817×10^{-3}	1.2247
506	1.2248	0.40815×10^{-3}	0.40818×10^{-3}	0.40815×10^{-3}	1.2248	0.40815×10^{-3}	0.40818×10^{-3}	0.40815×10^{-3}	1.2248
507	1.2249	0.40810×10^{-3}	0.40812×10^{-3}	0.40810×10^{-3}	1.2249	0.40809×10^{-3}	0.40812×10^{-3}	0.40819×10^{-3}	1.2249
508	1.2266	0.40879×10^{-3}	0.40882×10^{-3}	0.40879×10^{-3}	1.2266	0.40879×10^{-3}	0.40822×10^{-3}	0.40879×10^{-3}	1.2266
509	1.2264	0.43321×10^{-3}	0.43324×10^{-3}	0.43321×10^{-3}	1.2264	0.43321×10^{-3}	0.43324×10^{-3}	0.43321×10^{-3}	1.2264
510	1.5000	0.001	0.001	0.001	1.500	0.001	0.001	0.001	1.500

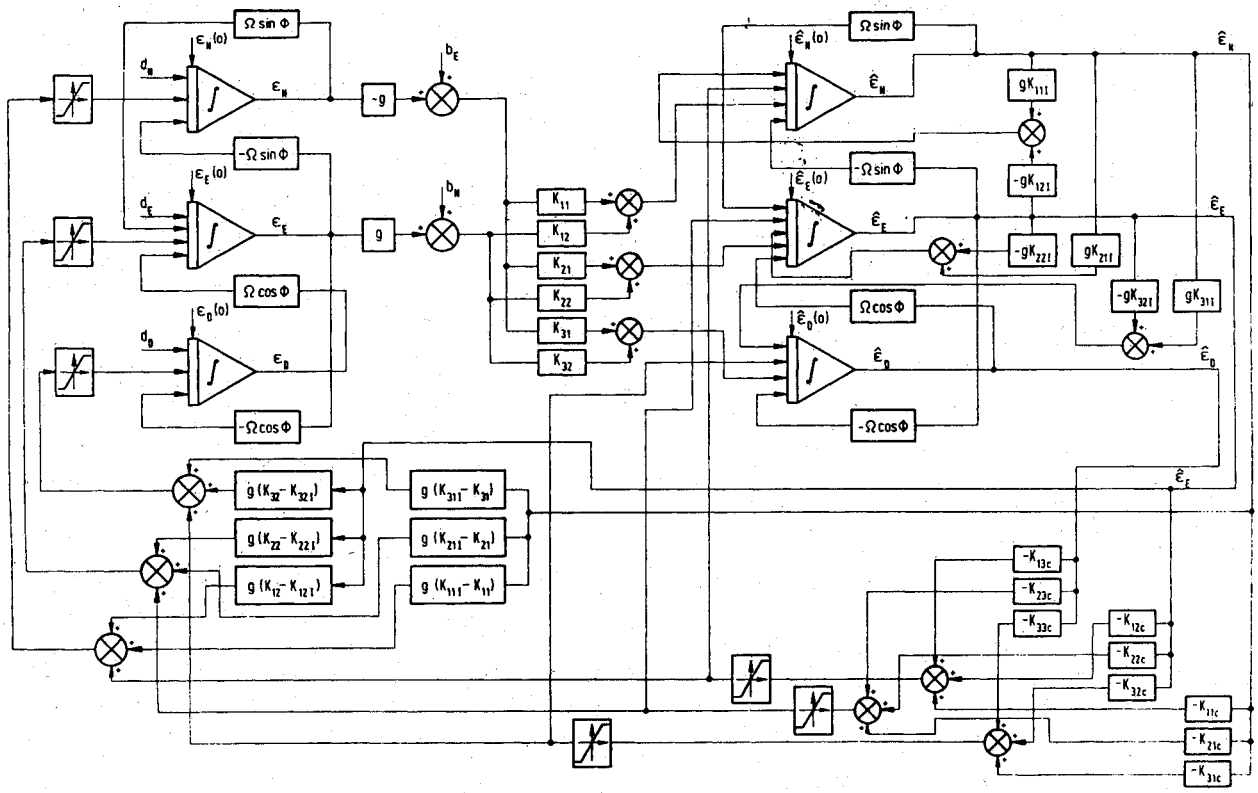

Fig. 4 Nonlinearity due to torque rate limit.

Essentially, $[n(n+1)]/2$ coupled nonlinear differential equations have been solved using the fourth-order Runge-Kutta technique for a step size of 1 sec. For $n = 7$, the case under consideration, the differential equations turn out to be 28. The filter performance has been verified using Monte-Carlo simulation; the details are given in Sec. VI. For closed-loop alignment, feedback controller gains are needed, the design of which has been discussed below.

Though the real-world model of the platform contains seven state variables, only the three misalignment angles E_N, E_E, and E_D can be regulated and driven to zero using the three independent gyro-torquer signals. Because of this practical consideration, it is quite logical to design a third-order controller. Referring to the problem formulation in Sec. II, the assumptions for the design are that 1) a quadratic performance index of the type $J_C(u)$ given by Eq. (12) is minimized, 2) Q_C is positive semidefinite and R_C is positive definite, 3) the control signals are not constrained, and 4) the control coupling matrix B represented in Eq. (1) is assumed to be an identity matrix.

Since the misalignment at the terminal time is very important and must be very low, Σ_{C_f} has been chosen as a nondiagonal matrix. Q_c and R_c also have been chosen as identity matrices.

The continuous Riccati equation has been solved backward from $t_f = 510$ sec with

$$\Sigma_{C_f} = \begin{bmatrix} 1.5 & .001 & .001 \\ .001 & 1.5 & .001 \\ .001 & .001 & 1.5 \end{bmatrix}$$

The transients have been observed from 510 sec to 505 sec. The gains attain a steady-state value from 505 sec to $t_0 = 0$. Table 1 presents the optimal control gains for closed-loop alignment. The weightage matrices have been changed to different values, and ultimately it has been found that the steady-state gains are insensitive to Q_c and R_c. Before implementing the scheme, it is necessary to check the closed-loop response characteristics and also the feedback torque rates. Often optimal feedback torque rates cannot be applied to the system because of torque rate limits imposed by platform hardware design.

The problem of torque rate limits cannot be solved at the time of designing the control gains. However, it can be taken care of by constraints on the controller: The simplest way is to introduce a linear saturation type of nonlinearity between the torquer and the controller.

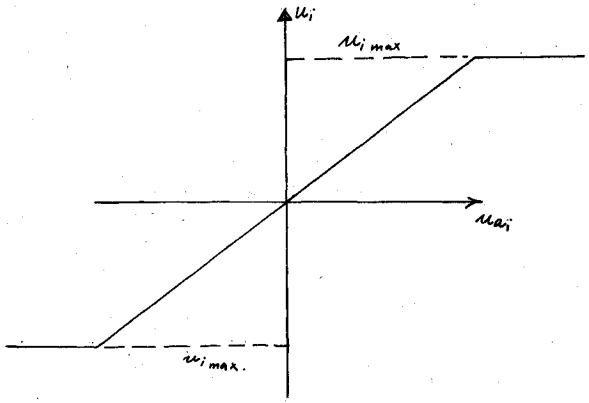

Fig. 5 Simulation layout for closed-loop alignment of inertial platforms.

Figure 4 presents this typical nonlinearity. Referring to Fig. 4, it can be seen that the applied torque rates u_{a_1}, u_{a_2}, and u_{a_3} can be obtained as

$$\begin{aligned} u_{a_i} &= u_i \qquad \text{if } u_i \le u_{i\max} \\ &= u_{i\max} \qquad \text{if } u_i > u_{i\max} \end{aligned} \tag{40}$$

Now, it is of interest to verify the design of the filter and controller for performance of the estimator interms of mean square estimation error and response characteristics of the controller. It is also of interest to check the performance of the system in the presence of torque rate nonlinearity. Carrying out these tasks using the actual platform hardware leads to prohibitive costs, but computer simulation can be considered as a tool for design verification. The integrated system simulation has been carried out for this system and is discussed in the next section.

VI. Simulation Studies

The noise signals have been simulated using standard random number generations.[15] Simulation studies have been conducted for 1) performance verification, and 2) minimizing speed of alignment. Figure 5 presents the simulation layout for closed-loop alignment of inertial platforms. For the normal Kalman filter controller configuration, the level misalignments have been estimated and controlled within 100 sec, whereas the azimuth misalignment error converged at about 500 sec. By using the filter configuration as given in Eq. (14), the azimuth alignment could be speeded up to 300 sec and, in some cases, 100 sec. The details are available in Refs. 12 and 13. From the initial azimuth misalignment of 378 arc min, the alignment accuracy obtained after 300 sec of alignment is of the order of 15 arc min in the presence of sway motion and 1.5 arc min without the sway motion.

VII. Summary

This paper has considered the application of optimal estimation and control concepts for the alignment of inertial platforms. The platform error model has been derived. The external sway disturbances have been modeled using second-order shaping filters from the experimental autocorrelation function. A reconfiguration of the filter is derived for speeding up azimuth alignment. Feedback control gains have been obtained by solving the matrix Riccati equation. The design has been verified using Monte Carlo simulation.

Appendix: Second-Order Shaping Filter

The second-order shaping filter is derived in Ref. 19 and is modified here to suit the autocorrelation function shown in Fig. 3.

The general exponential cosine autocorrelation function can be written

$$\phi(\tau) = \frac{\sigma^2}{\cos\eta} e^{-\xi\omega_n|\tau|}\cos(\omega|\tau| - \eta) \tag{A1}$$

where $\omega = \omega_n[1-\xi^2]^{\frac{1}{2}}$. The correlation function property $\phi(\tau) \le \phi(0)$ dictates that $\eta \le \alpha$, where

$$\alpha = \tan^{-1}\left\{\frac{\xi}{[1-\xi^2]^{\frac{1}{2}}}\right\} \tag{A2}$$

The power spectral density function is

$$G(\omega) = \frac{(a^2\omega^2 + b^2)/2\pi}{\omega^4 + 2\omega_n^2(2\xi^2 - 1)\omega^2 + \omega_n^4} \tag{A3}$$

where

$$a^2 = \frac{2\sigma^2}{\cos\eta}\omega_n\sin(\alpha - \eta) \tag{A4}$$

$$b^2 = \frac{2\sigma^2}{\cos\eta}\omega_n^3\sin(\alpha + \eta) \tag{A5}$$

For linear systems, the input/output relation indicates

$$G(W) = \|F(jW)\|^2 G_{ii}(W) \tag{A6}$$

If the system input $w_s(t)$ is white noise, with correlation function $\delta(\tau)$, and spectral density $G_{ii}(\omega) = 1/2\pi$, then for the power spectrum given by Eq. (A3) can be obtained if $F(s)$ is given by

$$F(s) = \frac{as + b}{s^2 + 2\xi W_n s + W_n^2} \tag{A7}$$

If the system is represented by a pair of first-order differential equations, then,

$$\begin{aligned} \dot{N}_1 &= AN_1 + BN_2 + Ew_{s_1} \\ \dot{N}_2 &= CN_1 + DN_2 + Fw_{s_1} \end{aligned} \tag{A8}$$

then the output $N_1(t)$ will exhibit the correlation function (A1), if the system coefficients satisfy the relationship,

$$\begin{aligned} E &= a \\ FB - ED &= b \\ A + D &= -2\xi\omega_n \\ AD - BC &= \omega_n^2 \end{aligned} \tag{A9}$$

Without any loss of generality, one can assume $\eta = 0$. Then Eq. (A1) becomes

$$\phi(\tau) = \sigma^2\exp^{-\xi\omega_n|\tau|}\cos(\omega|\tau|) \tag{A10}$$

Assuming $A = 0$ and $B = 1$,

$$D = -2\xi W_n,\ E = a,\ e = -W_n^2,\ F = b - 2a\xi W_n \tag{A11}$$

If the spectral density of the white-noise W_{s_1} is $2\beta\sigma^2$ instead of $1/2\pi$, then the sway model used in Eq. (34) results, which is shown in Ref. 16.

Acknowledgments

The author would like to thank Dr. H. Winter and Dr. B. Stieler of DFVLR, Braunschweig, West Germany, for fruitful discussions and data. Thanks are due Mr. Eugene Lefferts, NASA Goddard Space Flight Center, and Dr. F. L. Markley, U.S. Naval Research Laboratory, for encouraging me to write this paper. The financial support given by the Alexander Von Humboldt Foundation and the National Research Council is gratefully acknowledged.

References

[1]Parwin, R.H., "Inertial Navigation Systems: Prelaunch Alignment," *IRE Transactions on Aerospace and Navigational Electronics*, Sept. 1962, pp. 141-145.

[2]Cannon, R.H. Jr., "Alignment of Inertial Guidance Systems by Gyrocompassing—Linear Theory," *Journal of the Aerospace Science*, Vol. 28, Nov. 1961, pp. 885-895.

[3]Hodson, A.E., "Optimal Leveling and Gyrocompassing of Inertial Systems," *IEEE Transactions on Aerospace and Navigational Electronics*, March 1963, pp. 18-26.

[4]Miller, B., "Faster Carrier Inertial Alignment Sought," *Aviation Week*, Nov. 21, 1966, pp. 105-119.

[5]Jurenka, F.D. and Leondes, C.T., "Optimum Alignment of an Inertial Autonavigator," *IEEE Transactions on Aerospace and Electronic System*, Vol. AES-3, Nov. 1967, pp. 880-888.

[6]Sutherland, A.A. Jr., "The Kalman Filter in Transfer Alignment of Inertial Guidance Systems," *Journal of Spacecraft and Rockets*, Vol. 5, Oct. 1968, pp. 1175-1180.

[7]Kouba, J.T., "Application of Kalman Filtering for the Alignment of Carrier Inertial Navigation Systems," *Theory and Application of Kalman Filtering*, AGARDograph 139, 1970, pp. 407-421.

[8]Crocker, E.B. and Rabins, L., "Application of Kalman Filtering Techniques to Strapdown System Initial Alignment," AGARDograph 139, 1970, pp. 493-512.

[9]Winter, H., "The Modelling Error Sensitivity of Digital Filters for the Alignment of Inertial Platforms," AGARD Conference Proceedings No. 116, Papers 21C-1 to 21C-15, Oct. 1972.

[10]Stieler, B. and Zenz, H.P., "On the Alignment of Platform and Strapdown Systems," Symposium Gyro Technology Bochum, FRG, Sept. 18/19, 1978.

[11]Vathsal, S., "The Modelling Error Compensation of Digital Filters for the Alignment of Inertial Platforms," DFVLR-FB 79-19, Braunschweig, FRG, NTIS HC A 03/MF, 1979.

[12]Vathsal, S., "Simulation Studies on Closed Loop Alignment of Inertial Platforms," DFVLR-IB 153-79/19, Braunschweig, FRG, May 1979.

[13]Vathsal, S., "Simulation of Inertial Platform Alignment with Aircraft Sway," DFVLR-IB 153-79/38, Braunschweig, FRG, Dec. 1979.

[14]Vathsal, S., "A New Configuration for Linear Filtering Problems," *IEEE Transactions on Automatic Control*, Vol. AC 25, Dec. 1980, pp. 1006-1007.

[15]Hull, T.E. and Dobell, A.R., "Random Number Generators", *SIAM Review*, Vol. 4, July 1962, pp. 230-254.

[16]Arthur Gelb, (ed.), *Applied Optimal Estimation*, MIT. Press, Cambridge, MA, 1974.

[17]*Avionics Navigation Systems*, edited by Myron Kayton and Walter R. Fried, John Wiley & Sons, Inc., New York, 1969.

[18]Lohl, "Statisticsche Analyses von Verrauschten Meßsignalen einer LN3 Tragheits Navigation Anlage in Standlauf" DFVLR, Braunschweig, FRG, IB 153-77/25, 1977.

[19]Fitgerald, R.J., "Filtering Horizon-Sensor Measurements for Orbital Navigation," *Proceedings of the AIAA Guidance and Control Conference*, Seattle, WA, Aug. 1966, pp. 500-509.